









<b>Publication Year</b>	2022
<b>Acceptance in OA @INAF</b>	2023-01-20T15:53:59Z
<b>Title</b>	NEAR: A New Station to Study Neutron-Induced Reactions of Astrophysical Interest at CERN-n_TOF
<b>Authors</b>	Gervino, Gianpiero; Aberle, Oliver; Bernardes, Ana Paula; Colonna, Nicola; CRISTALLO, Sergio; et al.
<b>DOI</b>	10.3390/universe8050255
<b>Handle</b>	<a href="http://hdl.handle.net/20.500.12386/32965">http://hdl.handle.net/20.500.12386/32965</a>
<b>Journal</b>	UNIVERSE
<b>Number</b>	8

## Article

# NEAR: A New Station to Study Neutron-Induced Reactions of Astrophysical Interest at CERN-n\_TOF

Gianpiero Gervino <sup>1,2,\*</sup>, Oliver Aberle <sup>3</sup>, Ana-Paula Bernardes <sup>3</sup> , Nicola Colonna <sup>4</sup>, Sergio Cristallo <sup>5,6</sup> , Maria Diakaki <sup>7</sup>, Salvatore Fiore <sup>8,9</sup> , Alice Manna <sup>3,10,11</sup>, Cristian Massimi <sup>10,11</sup> , Pierfrancesco Mastinu <sup>12</sup>, Alberto Mengoni <sup>3,11,13</sup> , Riccardo Mucciola <sup>6,14</sup>, Elizabeth Musacchio González <sup>12</sup>, Nikolas Patronis <sup>3,15</sup>, Elisso Stamati <sup>3,15</sup> , Pedro Vaz <sup>16</sup> and Rosa Vlastou <sup>7</sup>

<sup>1</sup> Department of Physics, University of Torino, 10124 Torino, Italy

<sup>2</sup> INFN, Sezione di Torino, 10125 Torino, Italy

<sup>3</sup> European Organization for Nuclear Research (CERN), 1211 Geneva, Switzerland; oliver.aberle@cern.ch (O.A.); ana-paula.bernardes@cern.ch (A.-P.B.); alice.manna@bo.infn.it (A.M.); alberto.mengoni@cern.ch (A.M.); nikolaos.patronis@cern.ch (N.P.); maria-elisso.stamati@cern.ch (E.S.)

<sup>4</sup> INFN, Sezione di Bari, 70126 Bari, Italy; nicola.colonna@ba.infn.it

<sup>5</sup> INAF, Osservatorio Astronomico d'Abruzzo, 64100 Teramo, Italy; sergio.cristallo@inaf.it

<sup>6</sup> INFN, Sezione di Perugia, 06123 Perugia, Italy; riccardo.mucciola@pg.infn.it

<sup>7</sup> National Technical University of Athens, 10682 Athens, Greece; maria.diakaki@cea.fr (M.D.); rosa.vlastou@cern.ch (R.V.)

<sup>8</sup> ENEA, Department of Fusion and Technology for Nuclear Safety and Security, 00044 Frascati, Italy; salvatore.fiore@enea.it

<sup>9</sup> INFN, Sezione di Roma, 00185 Roma, Italy

<sup>10</sup> Department of Physics and Astronomy, University of Bologna, 40127 Bologna, Italy; cristian.massimi@bo.infn.it

<sup>11</sup> INFN, Sezione di Bologna, 40127 Bologna, Italy

<sup>12</sup> INFN, Laboratori Nazionali di Legnaro, 35020 Legnaro, Italy; pierfrancesco.mastinu@lnl.infn.it (P.M.); emg@lnl.infn.it (E.M.G.)

<sup>13</sup> ENEA, Department of Fusion and Technology for Nuclear Safety and Security, 40129 Bologna, Italy

<sup>14</sup> Dipartimento di Fisica e Geologia, Università di Perugia, 06123 Perugia, Italy

<sup>15</sup> Department of Physics, University of Ioannina, 45110 Ioannina, Greece

<sup>16</sup> Instituto Superior Técnico, 1049-001 Lisbon, Portugal; pedro.vaz@cern.ch

\* Correspondence: gervino@to.infn.it



**Citation:** Gervino, G.; Aberle, O.; Bernardes, A.-P.; Colonna, N.; Cristallo, S.; Diakaki, M.; Fiore, S.; Manna, A.; Massimi, C.; Mastinu, P.; et al. NEAR: A New Station to Study Neutron-Induced Reactions of Astrophysical Interest at CERN-n\_TOF. *Universe* **2022**, *8*, 255. <https://doi.org/10.3390/universe8050255>

Academic Editor: Fridolin Weber

Received: 29 March 2022

Accepted: 19 April 2022

Published: 20 April 2022

**Publisher's Note:** MDPI stays neutral with regard to jurisdictional claims in published maps and institutional affiliations.



**Copyright:** © 2022 by the authors. Licensee MDPI, Basel, Switzerland. This article is an open access article distributed under the terms and conditions of the Creative Commons Attribution (CC BY) license (<https://creativecommons.org/licenses/by/4.0/>).

**Abstract:** We present NEAR, a new experimental area at the CERN-n\_TOF facility and a possible setup for cross section measurements of interest to nuclear astrophysics. This was recently realized with the aim of performing spectral-averaged neutron-capture cross section measurements by means of the activation technique. The recently commissioned NEAR station at n\_TOF is now ready for the physics program, which includes a preliminary benchmark of the proposed idea. Based on the results obtained by dedicated Monte Carlo simulations and calculation, a suitable filtering of the neutron beam is expected to enable measurements of Maxwellian Averaged Cross Section (MACS) at different temperatures. To validate the feasibility of these studies we plan to start the measurement campaign by irradiating several isotopes whose MACS at different temperatures have recently been or are planned to be determined with high accuracy at n\_TOF, as a function of energy in the two time-of-flight measurement stations. For instance, the physical cases of  $^{88}\text{Sr}(n,\gamma)$ ,  $^{89}\text{Y}(n,\gamma)$ ,  $^{94}\text{Zr}(n,\gamma)$  and  $^{64}\text{Ni}(n,\gamma)$  are discussed. As the neutron capture on  $^{89}\text{Y}$  produces a pure  $\beta$ -decay emitter, we plan to test the possibility to perform activation measurements on such class of isotopes as well. The expected results of these measurements would open the way to challenging measurements of MACS by the activation technique at n\_TOF, for rare and/or exotic isotopes of interest for nuclear astrophysics.

**Keywords:** n\_TOF; NEAR; neutron activation; nuclear astrophysics; s-process; r-process

## 1. Introduction

Understanding our universe from the basic laws of nature is an ambitious goal involving many disciplines in physics. One key ingredient is nuclear astrophysics, with its focus on explaining energy production and chemical evolution in the universe, topics that are coupled through nuclear reactions that transform elements and may also release (or absorb) energy. In this context, neutron-induced reactions play a relevant role for the Big Bang and stellar nucleosynthesis. In addition, they are also important in classical nuclear physics topics, as symmetry-breaking effects in compound nuclei, the study of nuclear-level densities and for applications in advanced nuclear technology. This last includes nuclear medicine, transmutation of nuclear waste and nuclear fuel cycle investigations.

With the aim of collecting nuclear data of interest to these topics, the neutron time-of-flight (TOF) facility n\_TOF [1] was built at CERN some 20 years ago. It is based upon the CERN Proton Synchrotron (PS), which accelerates protons up to 20 GeV/c in bunches of up to  $10^{13}$  protons. Impinging on a massive Pb block surrounded by a water layer acting as moderator [2], each proton produces hundreds of neutrons. This makes n\_TOF an intense white spallation neutron source, with neutron kinetic energies from a few milli-eV to several GeV. It is important to recall that several white neutron sources (called white because they deliver beams of neutrons over a wide range of energies) are operating worldwide, each of them with specific characteristics and features, depending on the specific user requests [3]. However, only a few of them are pulsed and optimized for high energy resolution time-of-flight measurements, as in the case of n\_TOF.

Two experimental areas, EAR1 and EAR2, are connected to the n\_TOF spallation source by flight paths of 185 m and 19 m, respectively. So far, cross-sections have been measured in both EAR1 and EAR2 experimental areas for more than a hundred reactions and the data have been successfully exploited in modelling stellar and primordial nucleosynthesis (see, for instance, refs. [4,5]).

The idea of expanding n\_TOF measurement capabilities suggested a third beam line able to take advantage of the extremely high neutron fluence expected at a position very close to the spallation target (of the order of 3 m). This new beam line would make it possible to perform activation measurements on extremely small mass samples and on radioactive isotopes with very short half lives. Several feasibility studies have been performed and, since July 2021, the new experimental area, called NEAR, has become operative at n\_TOF.

The number of neutrons at the target position at NEAR is on average increased by a factor of  $\approx 100$  with respect to the EAR2 beam line and a factor  $\approx 4000$  with respect to EAR1. Since NEAR can operate in parallel with EAR1 and EAR2, it will contribute to a substantial improvement in experimental opportunities. In fact, we strongly believe that NEAR will allow us to investigate neutron-induced reactions which were not previously accessible.

In this article we report some results from the extensive Monte Carlo simulations that have been performed to optimize the characteristics of the NEAR neutron beam, in terms of neutron intensity and energy distribution for various combinations of collimators, moderators and filtering system. The adopted technical solutions and the achieved neutron beam characteristics are presented and discussed. In particular, we show that with a suitable choice of filter material and dimension, a Maxwellian-like neutron spectrum could be produced in the energy range of interest to stellar evolution investigations and Big Bang nucleosynthesis (i.e.,  $kT \approx \text{keV}$ ). In more detail, Maxwellian Average Cross Sections (MACS) can be measured by very thin targets ( $\approx \mu\text{g}/\text{cm}^2$ ), this feature being of key importance for radioactive isotopes and rare materials. In addition, the activation method can be applied on isotope radioactive targets of very short half-life, down to a few days—never measured before at n\_TOF. A new dedicated laboratory for activity measurements of  $\gamma$  and  $\beta$  rays (also referred to as  $\gamma$ -ray Spectroscopy Experimental Area or GEAR) is being equipped and soon will be made available.

An important advantage of NEAR, beside the presence of the activation laboratory, is its proximity to the ISOLDE facility, from which sample material to be irradiated could be

produced. This synergy has been already recently established [6] while its full exploitation is presently under study.

## 2. Stellar Evolution Investigations

Optical observations of stars reveal their element abundances. It is well-established that old stars belonging to the Galactic Halo are metal-poor (following the convention in astronomy that all elements above helium are metals) and that their heavy element (i.e., heavier than iron) distribution is mostly attributable to the main component of the rapid neutron capture process (the so-called *r* process [7]). For instance, the relative abundances for elements above barium fit well with *r*-process abundances deduced for solar-system material (see, e.g., [8]), but for lighter elements there are differences that could prove the presence of a second, so-called “weak”, *r* process. The question is open, and a better and refined understanding of this topic may come from the detailed study of the slow neutron capture process (the so-called *s* process; see e.g., [9]). Such a process appears later in the chemical evolution of our Galaxy, when Asymptotic Giant Branch (AGB) stars start polluting the interstellar medium [10]. An additional contribution to the *s*-process (the so-called weak *s*-process) comes from the quiescent burning phases of massive stars [11]. Overall, the *s*-process is responsible for the production of about half the cosmic elements heavier than iron.

Besides spectroscopic observations, a source of extremely precise data, precious to constrain stellar models, comes from pre-solar grains embedded in primitive meteorites. Those dust particles are relics of ancient stars that evolved prior to the formation of the Solar System, being trapped in minor bodies of the early Solar System (which later fell to the Earth). The extraction of isotopic ratios for many different grains represents a breakthrough in the field (e.g., [12,13]). In fact, such detailed information about isotope abundance can constrain the astrophysical conditions in which the grains were formed.

During *s*-process nucleosynthesis, neutron captures mostly occur on stable isotopes, because the unstable ones decay to their stable isobars before capturing a neutron. At higher temperatures, reactions involving radioactive nuclei become more important, with neutron captures possibly competing with the corresponding  $\beta$  decays (opening branchings in the *s*-process path). Unfortunately, the measurement of neutron capture cross sections on unstable isotopes is a very difficult task, due to the lack of a large enough quantity of the radioactive sample and of its intrinsic radioactivity. Both problems could be potentially overcome at NEAR station.

Another interesting field which could be approached at the NEAR station is the study of moderately neutron-rich unstable isotopes, lying on the right side of the  $\beta$  stability valley (i.e., with 1 to 6–7 more neutrons with respect to the most *n*-rich stable isotope). Recent works in the field of stellar spectroscopy (with relative theoretical interpretations) brought back the existence of a third neutron-capture process with intermediate neutron densities (*i*-process:  $N_n \approx 10^{14}$ – $10^{17}$  cm<sup>−3</sup>), which are intermediate between the *s*-process ( $N_n \approx 10^7$  cm<sup>−3</sup>) and the *r*-process ( $N_n > 10^{21}$  cm<sup>−3</sup>). The hosting object(s) of such a process has (have) not still been unequivocally identified (low-mass low-metallicity stars [14,15], Rapidly Accreting White Dwarfs [16], fast-rotating massive star experiencing a jet-like explosion [17]). Regardless of the stellar object, neutron capture cross sections on those unstable isotopes, which are currently only derived theoretically, need to be known with enough accuracy. The NEAR station will play a relevant role in this topic. Actually, theoretical studies on another nucleosynthesis process will benefit from this effort: the so-called *n*-process. The latter is at work during the explosive phase of massive stars, when the Supernova shock passes through the He-shell region, triggering a large production of neutrons in a very short timescale [18].

On a longer timescale, the NEAR station could potentially provide a breakthrough in our current knowledge of the *r*-process, by providing neutron-induced fission cross sections on short-lived unstable actinides. As a matter of fact, an exciting report on quantitative calculations of the *r* process suggests that nuclear fission, and in particular neutron-induced

fission, might play a very important role for the dynamics in later stages of the  $r$  process [19]. To that purpose, it is important to stress that all neutron-induced fission cross sections on short-lived unstable isotopes are derived theoretically.

In conclusion, modelling the evolution of stars and their sometimes-violent death requires information coming from different and often distant research fields. It is akin to assembling a giant multi-dimensional puzzle, but one in which the pieces have first to be found. Some researchers concentrate on finding these pieces, while others focus on how to fit them together to form a coherent picture. However, we have still not identified the important ingredients for all stellar events. The NEAR facility could successfully cast new light on some nuclear aspects related to the above-mentioned studies. In one of the following paragraphs we relate about the first planned measurements of interest to nuclear astrophysics, needed to characterize the newly established experimental area.

### 3. The n\_TOF NEAR Station Beam Line: A Brief Overview

As already mentioned, the neutron time-of-flight (n\_TOF) facility at the European Laboratory for Particle Physics (CERN) is a neutron source able to provide high-intensity pulsed white-spectrum neutrons covering almost 11 orders of magnitude, from thermal neutrons to several GeV. Since July 2021, a new experimental area called NEAR has been made available. Located at the end of a horizontal beam line, NEAR is only 3 m from the spallation target, see Figure 1.

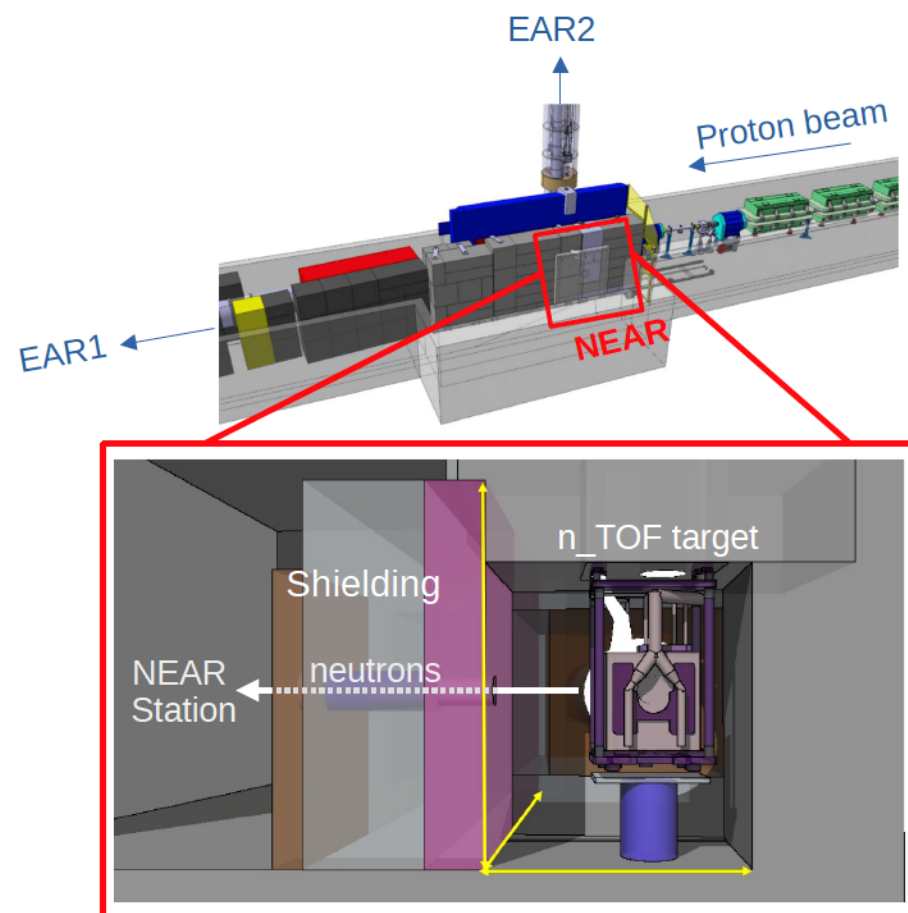


**Figure 1.** Layout of the n\_TOF Facility. A high-intensity proton beam from the CERN's Proton Synchrotron collides with a pure lead target, producing neutrons that travel along three flight paths toward the experimental areas: EAR1, EAR2 and NEAR. EAR1 is located 185 m from the target, EAR-2 is located 19 m above the target and NEAR at 3 m.

The new beam line was conceived to study the neutron–nucleus interactions of interest for nuclear astrophysics, nuclear technology and medical research applications that require a highest neutron fluence and that were, up to now, outside the performance of the two already existing experimental areas. The PS accelerator delivers proton bunches with a minimum pulse period of 1.2 s and the maximum average intensity allowed on target is  $1.67 \times 10^{12}$  protons per second, corresponding to an average power on the spallation target of 5.4 kW. With a pulse duration of 7 ns (rms), this yields a peak deposited power of 1.8 TW. The proton beam size on target is around 15 mm (rms).

It is worth recalling that a new spallation target (also referred to as third-generation spallation target) able to couple with the high power deposition has been installed during the Long Shutdown (a 3-year stop of the CERN accelerators that ended in the summer of 2021). High-purity lead has been chosen as the core material owing to its very good performances in terms of reduced photon background and neutron production. The new assembly is shown, in exploded view, in Figure 2: housed inside a stainless steel vessel, six lead slices are cooled by gaseous nitrogen and are supported by precisely machined anticreep plates [2]. These are made of aluminum alloy and include the channels through which the cooling fluid flows. The cooling gas is distributed through two main channels inside a cradle made from aluminum alloy, which supports the lead core from below. The bond between the stainless steel vessel and the aluminum cradle is obtained by an explosive-bonded joint technique where two different metals are forced together under very high pressure.

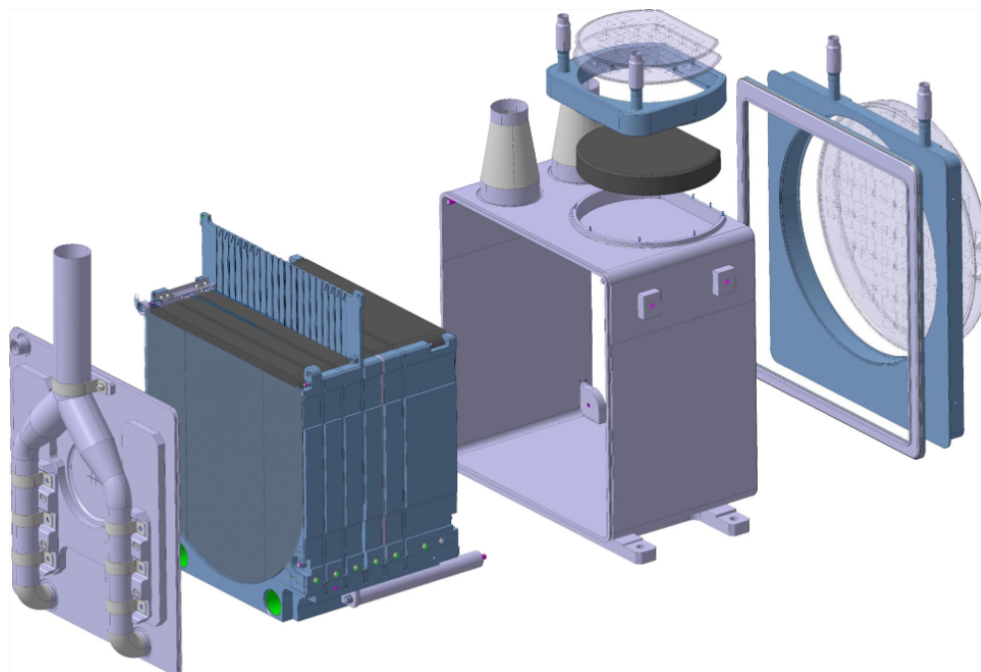


**Figure 2.** Exploded model of the target. The cooling nitrogen gas flows through the channels machined into the anticreep plates. The inner core is enclosed in an AISI 316L stainless steel vessel (figure from ref. [2]).

The neutron flux emerging from the spallation target is online monitored by a set of 10 self-powered neutron detectors (SPNDs) placed around the spallation target, divided in two stations on both sides of the target with respect to the beam direction (Figure 3). SPNDs are rugged miniature detectors, capable of operating without any bias voltage by exploiting the direct detection of secondary electrons. With a typical diameter of a few mm, they are usually built in a coaxial configuration with a core (emitter), an electrically conductive collector and an insulating medium of aluminum oxide between them. Different reactions can take place inside SPNDs, inducing a measurable current through the emission



of electrons. These electrons can be emitted either by the  $\beta$ -decays of neutron-induced daughter nuclei, or by Compton or photoelectric interactions of photons. To monitor the neutron and gamma flux from the spallation target, SPNDs with a central emitter made of Rh, Co, Pt, V, Inconel (the latter for background current evaluation) have been chosen. The different materials allow us to disentangle between the signals induced by prompt gamma, prompt and delayed neutron response [20].



**Figure 3.** The n\_TOF spallation target during the installation phase. The right side station with 5 SPNDs is visible at the centre of the photo.

At present, the neutron beam arrives at the NEAR experimental area through a hole in the shielding wall and no moderator is present. However, the study of the effect of different moderators (for instance,  $\text{AlF}_3$ ,  $\text{D}_2\text{O}$ ,  $\text{BeO}$ , ...) to be added inside the target hall in the near future (see Figure 4) is ongoing.

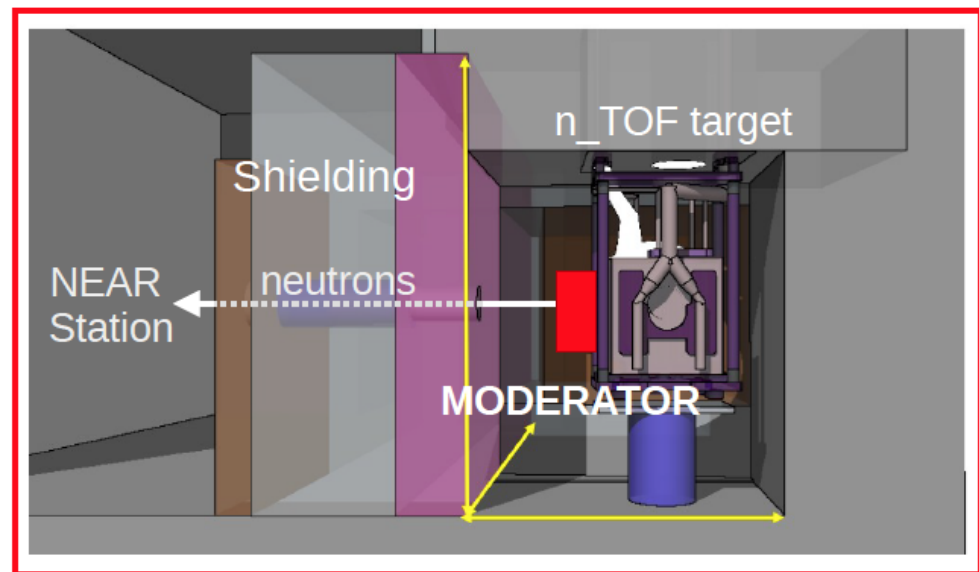


**Figure 4.** Schematic drawing of the spallation target and the possible position of a moderator (block in red).

A moderator is needed to reduce the high energy components ( $E_n > 1$  MeV) of the neutron spectrum and then to shape the neutron energy distribution as a Maxwellian-like distribution.  $(n, \gamma)$  cross sections typically decrease rapidly above 1 MeV.

In addition, out of this target station (see Figure 5) boron and cadmium slices (also referred to as filters) can be placed in the beam to remove low-energy neutrons. As an example Figure 6 shows the expected neutron flux at NEAR (i.e., at the position of the irradiation for activation measurements) with and without a 1.5 cm-thick filter containing  $^{10}\text{B}$ .

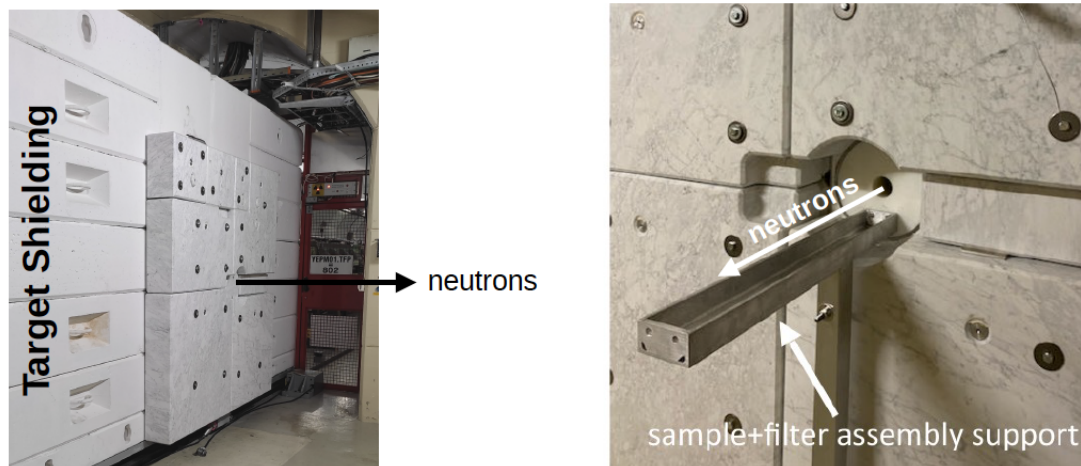


**Figure 5.** View of the concrete and marble shielding around the spallation target (**left panel**) and the zoom on the irradiation position at NEAR (**right panel**).



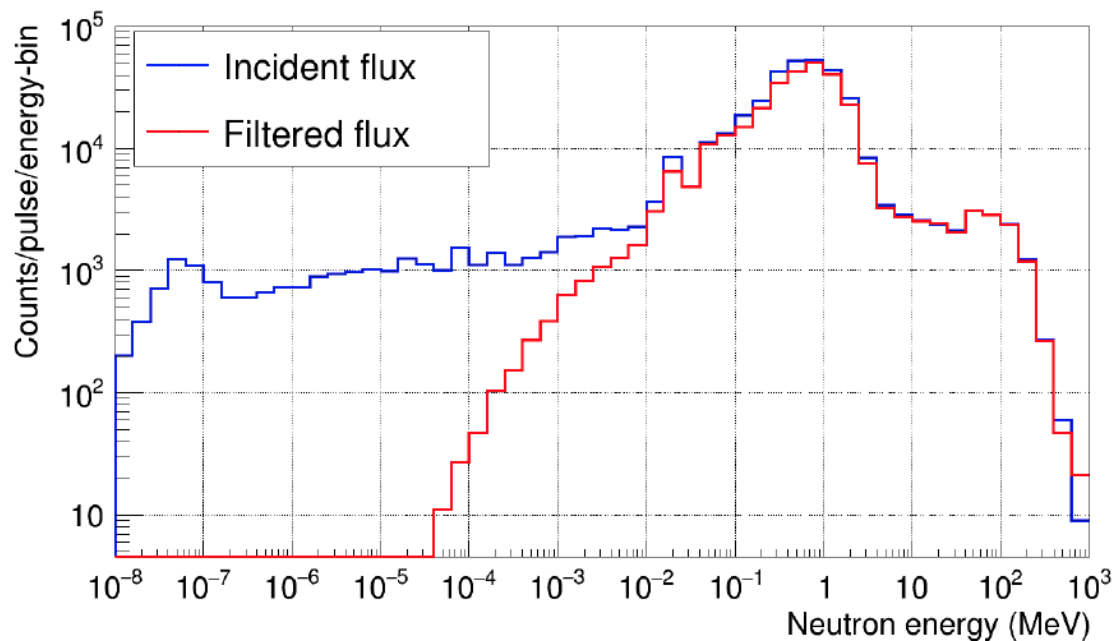


**Figure 6.** Expected neutron flux at the irradiation position with and without a 1.5 cm-thick boron filter.

It is also necessary to reduce efficiently the effect of back-scattered neutrons from the wall of the NEAR station; for this purpose, the filter made of a slab of material requires specific modification. According to our simulations, a suitable filter consists of a boron carbide  $B_4C$  cylinder highly enriched in  $^{10}B$ . Figure 7 shows the absorption cross section of  $^{10}B$  and C.

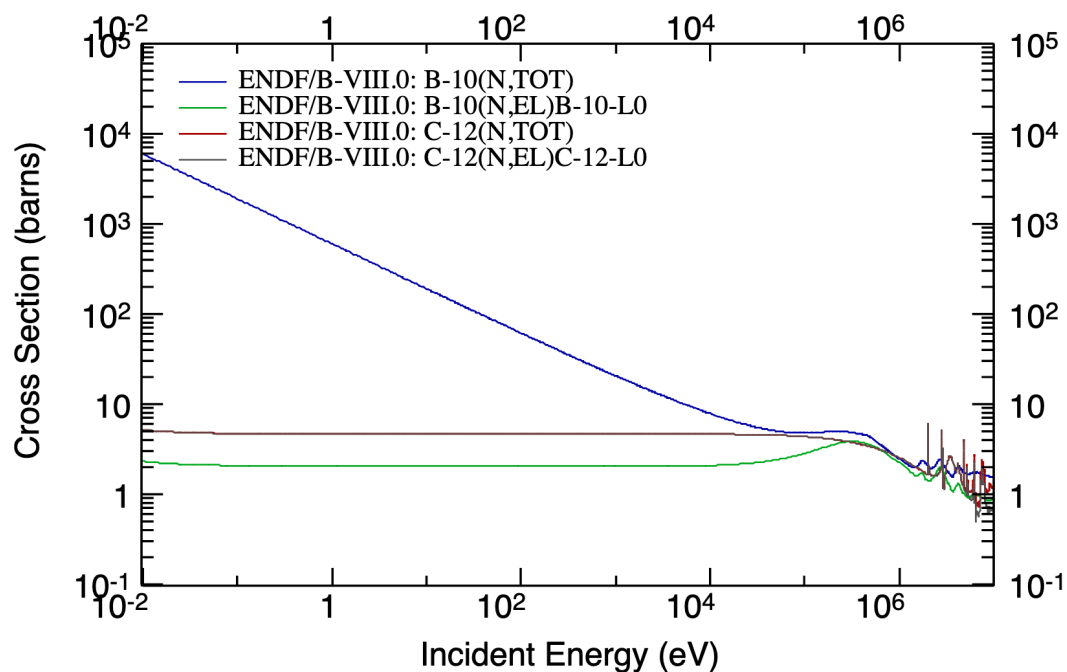


**Figure 7.** Neutron-induced total and elastic cross sections of  $^{10}B$  and  $^{12}C$ . The absorption cross section of  $^{10}B$  and  $^{12}C$  is, respectively, orders of magnitudes higher and lower than the elastic cross section. Consequently,  $^{10}B$  is very effective to absorb low energy neutrons, while  $^{12}C$  can moderate them, thus reducing the initial kinetic energy. It is worth noticing that the elastic cross section on  $^{12}C$  almost coincides with the  $n+^{12}C$  total cross section.

MC simulations show that the neutron energy distribution changes sizeably as a function of the cylinder's thickness (from 0.5 to 2 cm), see Figure 6. We have also investigated the idea of performing several irradiations in parallel, by using a cylinder with a radius of 5 cm to house samples of 1 cm radius. The neutron energy distribution inside the cylinder slightly changes with position, along its radius and thickness: while the total number of neutrons reduces by approximately 30%, moving from the center to the position at 3 cm from the center, the shape of the energy distribution does not change appreciably. To reduce this effect, the samples are located in the same plane (i.e., experiencing the same moderator thickness) with respect to the beam axis and symmetrically from the axis.

In summary, MC simulations have indicated that, with a suitable choice of filter material and dimension, a Maxwellian-like neutron spectrum could be produced (see Figure 8), corresponding to thermal energies in the range of astrophysical interest (from a few keV to a few tens of keV) that would allow us to derive MACS by means of activation technique. The role of the  $B_4C$  on the thermal and epithermal region is apparent (see Figure 6). In fact, low-energy neutrons are absorbed (or moderated and eventually absorbed) inside the  $B_4C$  cylinder. As a result, the mean energy of the distribution is shifted at higher energies and a large fraction of the lower energy neutrons is lost. The advantage is that the neutron energy distribution presents a dominant peak, roughly shaped to resemble a Maxwell–Boltzmann distribution, as showed in Figure 8. Although not completely satisfying, mainly because of the tail at high energies, this preliminary configuration can already provide strong indication on the effectiveness of the proposed setup. With future upgrades we are confident to improve the agreement between shaped and expected Maxwell–Boltzmann distributions.

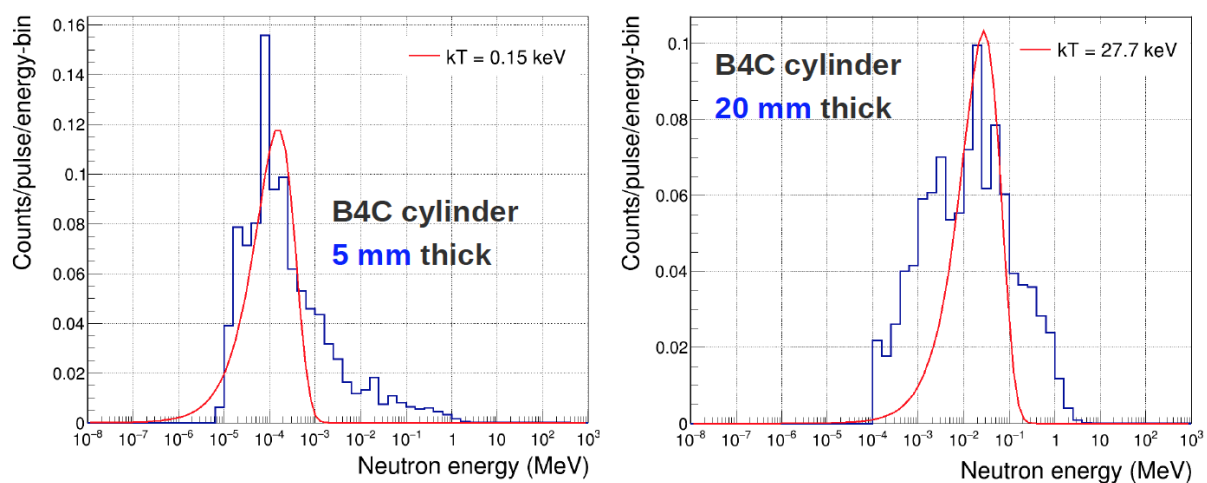


**Figure 8.** Expected neutron flux shape in the NEAR Station area at the measuring position with 0.5 cm (left panel) and 2 cm (right panel)-thick boron layers, respectively. The spectra are compared to a Maxwellian spectrum of thermal energy  $kT = 0.15$  keV and  $kT = 27.7$  keV respectively.

#### 4. MACS cross Section by Activation Method

The limits of the TOF technique in measuring small stellar cross sections and/or small mass samples are well known [21]. Therefore, if applicable, the higher sensitivity of the activation method would be preferable in these cases. With this latter method, the activity  $A$  of an irradiated sample can be related to the decay rate (i.e., decays per unit time:  $A = \Delta N / \Delta t$ , where  $\Delta N$  is the number of decays that occur in time  $\Delta t$ ). In fact, several radioactive nuclei are present in a neutron-irradiated sample, eventually decaying by  $\gamma$  and/or  $\beta$  emission.

On the other hand, the activity of an irradiated sample is directly proportional to the amount of the radionuclides present in the sample (that in turn is strictly linked to the neutron capture cross section value), and is inversely proportional to its half-life.

The radiation emitted by the produced unstable nuclei can be detected after an extended period (of the order of 2 weeks, corresponding to  $\approx 10^{13}$  neutrons on target) of

irradiation via their decay signatures and then the determination of MACS cross sections, extremely helpful for modelling the advanced phases of massive stars in which very large temperatures are reached. We refer to ref. [21] for a detailed description of the observables and corrections.

The new GEAR laboratory is equipped with two spectrometers for  $\gamma$  and  $\beta$  spectroscopy with lead-copper shielding. The available instrumentation will be used to measure the induced activity.

Accurate  $\gamma$ -ray spectroscopy requires (i) high detection efficiency, (ii) high energy resolution and (iii) the lowest possible background. In order to satisfy these conditions, we use a HPGe (High Purity Germanium) spectrometer electrically cooled and with a relative efficiency as high as 60%. In addition, the HPGe window is made of carbon epoxy, thus enabling the measurement of  $\gamma$  rays in a very wide energy spectrum ranging from a few keV up to 10 MeV, see Figure 9.

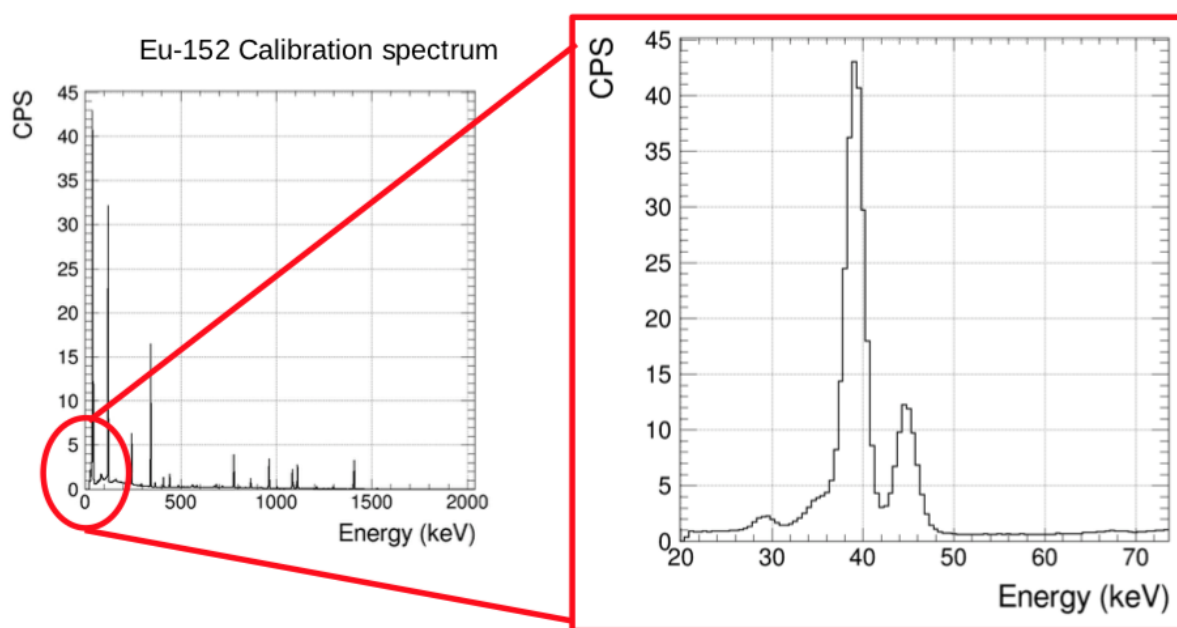


**Figure 9.** Example of  $\gamma$ -ray spectrum acquired with the HPGe detector and zoom on the X-ray lines from  $^{152}\text{Eu}$  calibration in the 20–70 keV energy region.

Furthermore, to optimize the background conditions as much as possible, the detector is installed and operated inside a specially designed lead shielding (CANBERRA 747). Accordingly, thanks to the high neutron flux of NEAR in combination with the high energy resolution and the low-background setup described above, we can perform high-accuracy studies on low-mass samples, even of the order of mg.

Apart from the standard  $\gamma$ -spectroscopy, special effort is being devoted to the feasibility study of  $\beta$  spectroscopy measurements. A possible detection set-up under investigation is based upon a couple of HPGe crystals, with 30% efficiency each, mounted very close face to face with the activated sample to be inserted in between (then covering more than 80% solid angle) or, alternatively plastic scintillators in almost  $4\pi$  geometrical setup.

At any depth in the sample, electrons or positrons are emitted isotropically with a continuum of energies up to the maximum energy  $E_{max}$ . Unlike the case of  $\gamma$  rays, which travel almost in straight line with a well-defined range,  $\beta$  particles travel along twisted trajectories that could end at any distance from the emission point inside the sample up to the continuous slowing down approximation range of  $\beta$  particles. To accurately evaluate the sample activity for  $\beta$  particle emission it is necessary to rely on the Monte Carlo method to correct the experimental spectra.

Finally, it is important to mention that the primary proton beam intensity for each delivered pulse is recorded, allowing us to reconstruct—in detail—the time dependence of the neutron flux throughout the irradiations. In fact, the knowledge of the experimental conditions during activation allow us to assess the corresponding correction factors to be applied [21]. Most importantly, the activated samples will be sandwiched between reference gold foils and placed inside NEAR, in front of the neutron beam. The  $^{197}\text{Au}(n,\gamma)$  reaction will be used as a reference cross section and therefore the results will be provided relative to it.

## 5. First Activation Measurement Campaign at NEAR and Their Physics Cases

In the following we describe and discuss the physics motivation of the next measurement campaign at the NEAR station using the activation method and exploiting the equipment available at GEAR. In particular, we aim at producing accurate experimental data for some reactions of special interest for the  $s$  process. Nevertheless, it is important to mention that the MACS of these elements have been already studied at n\_TOF with the time-of-flight technique. Therefore, this measurement campaign aims at benchmarking the experimental facility. In more detail, we proposed to verify the MC calculations by measuring the spectrum-averaged cross section at three different temperatures (ranging from a few keV up to 100 keV), for isotopes whose energy-dependent cross sections have recently been measured or are planned to be measured in near future at the two time-of-flight measurement stations EAR1 and EAR2. Beside  $^{197}\text{Au}$  [22–24], that will be used both as a benchmark and reference for the other isotopes, possible candidates are  $^{64}\text{Ni}$ ,  $^{76}\text{Ge}$  [25],  $^{88}\text{Sr}$ ,  $^{89}\text{Y}$ ,  $^{94}\text{Zr}$  and  $^{140}\text{Ce}$  [26]. Hereafter, examples of physics cases are discussed.

### 5.1. The Case of $^{88}\text{Sr}(n,\gamma)$

With its very small neutron capture cross section,  $^{88}\text{Sr}$  largely affects  $s$ -process nucleosynthesis: its large abundance in the Solar System testifies that. As a matter of fact, Sr is mostly synthesized by the  $s$  process in AGB stars, its contribution by  $r$  process being limited to some percent of the total solar abundance [8,27]. Apart from that, it is important to stress that, after the discovery of a pair of neutron stars merging in 2017, dubbed GW170817, telescopic observations from Earth revealed a spectroscopic feature linkable to strontium [28]. The discovery of strontium lines in kilonovae remnants was one of the first success of the synergy collaboration between spectral observations, gravitational waves hunting and nuclear astrophysics, giving the start to what now is known as multimessenger astrophysics.

Sr belong to the first peak of the  $s$ -process, the so-called “ $1s$ ” (light- $s$ ) peak, which is routinely used to compare theoretical models to observations.  $^{88}\text{Sr}$  has a magic number of neutrons ( $N = 50$ ), which implies that its neutron-capture cross section is lower than those of its neighbouring nuclei. As a result,  $^{88}\text{Sr}$  acts as a bottleneck in the neutron-capture path, constraining the value of the total neutron flux necessary to proceed to the production of heavier elements up to the second  $s$ -process peak, corresponding to the next bottleneck with neutron magic number of 82 (defining the heavy- $s$  “ $hs$ ” index). Consequently,  $^{88}\text{Sr}$  influences not only the abundance of neighbouring isotopes, but the whole  $s$ -process abundance distribution. As a final remark, the Sr abundance in stars is relatively easy to derive from high-resolution spectra thanks to its strong lines. In fact, they have been used extensively to constrain stellar models [29] and even astrophysical scenarios, e.g., related to the origin of chemical anomalies in ancient globular clusters [30]. Moreover, Sr isotopic ratios in SiC grains is strongly dependent upon the  $^{88}\text{Sr}(n,\gamma)$  cross sections [31,32].

On the other hand, the  $r$  process only takes place in nature in extreme environments where atoms are bombarded by a large number of neutrons, and recent works suggest that a likely source of  $r$ -process elements could be the catastrophic aftermath of mergers between neutron stars, which are the superdense cores of stars left behind after cataclysmic, explosive star deaths known as supernovas. The neutron star resulting from their gravitational pull is strong enough to crush protons and electrons together to form neutrons [8]. In this context,



stellar models require accurate stellar cross section (i.e., MACS) to reproduce the observed element abundances. Astrophysicists expected to find heavier *r*-process elements when looking at a kilonova [33]. The experimental details for this reaction are given below, along with the  $^{89}\text{Y}(n,\gamma)$  reaction.

### 5.2. The Case of $^{89}\text{Y}(n,\gamma)$

Together with  $^{88}\text{Sr}$ ,  $^{89}\text{Y}$  shares the same physical case. Indeed, both are bottlenecked in the *s*-process reaction path, strongly constraining the efficiency for the production of heavier elements up to the second *s*-process peak (associated to the next bottleneck that corresponds at Ba, La, Ce, i.e., neutron magic number of 82). The Solar System abundances of Y, as well as Sr and Zr, all having a magic number of neutrons ( $N = 50$ ), are relatively high. The only stable isotope of Yttrium is  $^{89}\text{Y}$  that is created by nucleosynthesis, mainly by the *s*-process (78%) inside pulsating red giant stars, and by the *r*-process (22%) during supernova explosions or the merger of compact objects. Any careful analysis of the observed abundance pattern in the nuclides mass range  $78 < A < 92$ , i.e., the decomposition according to the various processes, can only be carried out on the basis of precise  $(n,\gamma)$  cross sections. In addition, Y has several applications in advanced nuclear technology and radiation measurement techniques. We remind that the quoted stellar cross section of  $^{88}\text{Sr}$  and  $^{89}\text{Y}$  at  $kT = 30$  keV in the literature spans from 5 to 13 mb and from 13 to 27 mb, respectively, these large variations being also related to the used experimental technique. The major complication with  $^{89}\text{Sr}$  and  $^{90}\text{Y}$  is that both  $\beta$  decays directly to the ground state of their daughter nuclei. In particular,  $^{89}\text{Sr}$  being a  $\beta$  pure emitter,  $\beta$  decays with a half-life of 50.52 d directly to the ground state, and therefore there are no associated  $\gamma$  transitions. However, the ejected electron has a maximum energy of 1502 keV, large enough to produce an experimental signature above the background. Similarly,  $^{90}\text{Y}$  undergoes a pure  $\beta^-$  decay to  $^{90}\text{Zr}$  with a half-life of 64.1 h and a decay energy of 2.28 MeV, corresponding to an average electron energy of 0.934 MeV. For sake of completeness,  $^{90}\text{Y}$  also produces 0.01% 1.7 MeV photons during its decay process to the  $J^\pi = 0^+$  state of  $^{90}\text{Zr}$ , followed by pair production. As already mentioned before, in these two cases the decays will be detected using a  $\beta$  spectrometer.

### 5.3. The Case of $^{94}\text{Zr}(n,\gamma)$

Zr is an element widely studied in nuclear astrophysics because of its key role in the *s*-process and nuclear technology [34]. It is closely linked to the first *s*-process peak in the solar-abundance distribution (according to recent theoretical studies, predicted *s*-process contributions to its solar abundance is 82% [8]). The comparison of AGB predictions to the Zr composition of single SiC data presents some problems, in particular the large  $^{92}\text{Zr}/^{94}\text{Zr}$  ratios measured in grains. One can argue that improved measurements of neutron-capture cross sections for the  $^{94}\text{Zr}$  isotope may help solving these problems and we plan to investigate it at NEAR with the aim to reach an accuracy around or better than 5%. In addition, the activation measurement of  $^{94}\text{Zr}$  is relevant outside nuclear astrophysics too. Ongoing research on  $k_0$ -standardized reactor neutron activation analysis [35] requires  $^{94}\text{Zr}(n,\gamma)$  data deduced from neutron irradiation. So far, measurements in irradiation facilities with significantly different spectral characteristics were discrepant far outside experimental uncertainties.  $^{95}\text{Zr}$  is a  $\gamma$ -ray emitter, with two main lines, 724 and 757 keV, and a half-life of 64.02 d.

### 5.4. The Case of $^{64}\text{Ni}(n,\gamma)$

A large fraction of nuclides in the Fe/Ni mass region is produced by the weak *s* process. In particular, the *s*-process nucleosynthesis takes place during core He-burning, when temperatures are high enough to activate the neutron source reaction  $^{22}\text{Ne}(\alpha,n)^{25}\text{Mg}$ . In this case neutron densities reach around  $10^6 \text{ cm}^{-3}$  and temperatures corresponding to  $kT = 26$  keV. The very same neutron source is later reactivated during C-Shell burning at temperatures of  $kT = 90$  keV. In this latter case, neutron densities are orders of magnitude

higher with peak densities up to  $10^{12} \text{ cm}^{-3}$ , resulting in a reaction flow slightly away from the nuclear stability valley. In this context, when  $^{63}\text{Ni}$  radioisotope is produced, the main reaction flow proceeds via subsequent neutron capture to  $^{64}\text{Ni}$ , bypassing the production of  $^{63}\text{Cu}$ .  $^{64}\text{Ni}$  is involved in both burning process He-Core and C-Shell. Clearly, how fast the  $^{64}\text{Ni}$  stable nucleus is turned into  $^{65}\text{Ni}$  by neutron capture depends upon its stellar  $(n, \gamma)$  cross section, and in addition it affects the abundances of all other isotopes following in the reaction chain (see, e.g., ref. [11]).

Another interesting feature related to nickel isotopic ratios is that they can be measured in presolar SiC grains: considering the high resolution of these laboratory measurements (less than 5%), an equivalent accurate determination of nuclear inputs is needed [36,37]. As a final remark, there are few and discrepant reported cross sections in literature (far outside the uncertainties that in this case amount of a great percent fraction), probably because of its small absolute value.  $^{64}\text{Ni}(n, \gamma)^{65}\text{Ni}$  requires a special consideration: this reaction is a challenge because of its short half-life (only 2.5 h) with a Q-value of 2137 keV, and we will then test the actual activity limit of the combination NEAR and GEAR lab. This could be a good opportunity to investigate the relation between half-life of the sample and reachable accuracy of the cross section determination. We expect to reach in this measurement campaign an accuracy of a few percent in all the measurements, apart from  $^{65}\text{Ni}$  that is hampered by its short half-life.

## 6. Activation Measurements at NEAR on a Mid- and Long-Term

In the previous Section we listed the first measurements that will be performed at NEAR, needed to characterize the experimental setup. Thus, such a list is intended to be non-exhaustive. As a matter of fact, we are planning to approach the neutron-rich side of the  $\beta$ -stability valley by measuring neutron captures on n-rich unstable isotopes. As already recalled in the Introduction, those data are fundamental for the analysis of s-process branchings and for studies involving processes with intermediate neutron densities ( $N_n \approx 10^{14} - 10^{17} \text{ cm}^{-3}$ ). Hereafter, we list just a couple of potential cases:

- $^{135}\text{Cs}(n, \gamma)$  &  $^{136}\text{Cs}(n, \gamma)$ : the competition between neutron captures and  $\beta$  decays of those unstable isotope determine the final surface abundance of  $^{136}\text{Ba}$  in AGB stars.  $^{136}\text{Ba}$  is an s-only isotope, in the sense that its entire cosmic production can be ascribed to the s-process: for this reason it is widely used (together with other s-only isotopes) to test the robustness of theoretical stellar models [8]. Its abundances is largely dependent from the branchings at  $^{135}\text{Cs}$  and  $^{136}\text{Cs}$ , thus the determination of their neutron capture cross sections is mandatory.
- $^{89}\text{Sr}(n, \gamma)$  &  $^{90}\text{Sr}(n, \gamma)$ : those unstable isotopes do not influence the main s-process neutron capture path but, with sufficiently large neutron exposures, their neutron capture may potentially by-pass the neutron-magic nuclei  $^{89}\text{Y}$  and  $^{90}\text{Zr}$ . This is a typical condition attained during the i-process, when up to six to seven neutron-rich nuclei far from the  $\beta$ -stability valley are produced [16]. Different light-s to heavy-s element distribution could be attained on the surface of the objects where the i-process is at work, with interesting consequences on the evaluation of the contribution of this process in the framework of the Galactic chemical evolution.
- $^{31}\text{Si}$ : the branching at this isotope determines the final  $^{32}\text{S}$  abundance in particular classes of pre-solar SiC grains (X grains, related to core-collapse supernovae [38], and AB grains, whose origin is still under debate [39]). In particular, the measured  $^{32}\text{S}$  excess is due to the radiogenic contribution from  $^{32}\text{Si}$ , that is strongly affected by the neutron capture cross section of the unstable  $^{31}\text{Si}$ . The latter is far from being precisely determined.

## 7. Conclusions

The upgrade of the n\_TOF neutron spallation source during the CERN shutdown in 2019–2020 has enabled the construction of NEAR, an irradiation station close to the neutron source. After the characterization of the neutron beam at NEAR, the n\_TOF collaboration is

proposing for the next future a series of measurements of astrophysical interest: we mention the s-process in AGB stars (5–30 keV neutron energy range) and s-process in massive stars (15–90 keV neutron energy range). In particular, a method has been proposed and described in this article to shape the neutron flux at NEAR so as to resemble a Maxwellian distribution at different temperatures.

Rare, radioactive or low-mass samples can be irradiated at NEAR (down to few ng/cm<sup>2</sup> thickness) and then the produced activity (we could consider samples with half-life up to few months) measured in the measurement station GEAR, hosted in a dedicated low-level underground laboratory equipped with shielded HPGe detectors and *beta* counters. This latter station is positioned close to the NEAR station (a few hundred meters away), thus allowing us to measure the activities of short-lived radioisotopes too.

The physics program of NEAR in the short- and mid-term, described in this article, consists of several activation measurements on stable and unstable isotopes. They are of interest to nuclear astrophysics and, in particular, to the study of the production of elements heavier than iron in the stars.

**Author Contributions:** All authors have equally contributed to this article. All authors have read and agreed to the published version of the manuscript.

**Funding:** This research received no external funding.

**Institutional Review Board Statement:** Not applicable.

**Informed Consent Statement:** Not applicable.

**Acknowledgments:** We acknowledge the n\_TOF collaboration.

**Conflicts of Interest:** The authors declare no conflict of interest.

## References

- Guerrero, C.; Tsinganis, A.; Berthoumieux, E.; Barbagallo, M.; Belloni, F.; Günsing, F.; Weiß, C.; Chiaveri, E.; Calviani, M.; Vlachoudis, V.; et al. Performance of the neutron time-of-flight facility n\_TOF at CERN. *Eur. Phys. J. A* **2013**, *49*, 27. [\[CrossRef\]](#)
- Esposito, R.; Calviani, M.; Aberle, O.; Barbagallo, M.; Cano-Ott, D.; Coiffet, T.; Colonna, N.; Domingo-Pardo, C.; Dragoni, F.; Franqueira Ximenes, R.; et al. Design of the third-generation lead-based neutron spallation target for the neutron time-of-flight facility at CERN. *Phys. Rev. Accel. Beams* **2021**, *24*, 093001. [\[CrossRef\]](#)
- Colonna, N.; Günsing, F.; Käppeler, F. Neutron physics with accelerators. *Prog. Part. Nucl. Phys.* **2018**, *101*, 177–203. [\[CrossRef\]](#)
- Günsing, F.; Aberle, O.; Andrzejewski, J.; Audouin, L.; Bécaries, V.; Bacak, M.; Balibrea-Correa, J.; Barbagallo, M.; Barros, S.; Bečvář, F.; et al. Nuclear data activities at the n\_TOF facility at CERN. *Eur. Phys. J. Plus* **2016**, *131*, 371. [\[CrossRef\]](#)
- Massimi, C.; Cristallo, S.; Domingo-Pardo, C.; Lederer-Woods, C. n\_TOF: Measurements of Key Reactions of Interest to AGB Stars. *Universe* **2022**, *8*, 100. [\[CrossRef\]](#)
- Damone, L.; Barbagallo, M.; Mastromarco, M.; Mengoni, A.; Cosentino, L.; Maugeri, E.; Heinitz, S.; Schumann, D.; Dressler, R.; Käppeler, F.; et al. <sup>7</sup>Be (n,p) <sup>7</sup>Li Reaction and the Cosmological Lithium Problem: Measurement of the Cross Section in a Wide Energy Range at n\_TOF at CERN. *Phys. Rev. Lett.* **2018**, *121*, 042701. [\[CrossRef\]](#) [\[PubMed\]](#)
- Cowan, J.J.; Sneden, C.; Lawler, J.E.; Aprahamian, A.; Wiescher, M.; Langanke, K.; Martínez-Pinedo, G.; Thielemann, F.K. Origin of the heaviest elements: The rapid neutron-capture process. *Rev. Mod. Phys.* **2021**, *93*, 015002. [\[CrossRef\]](#)
- Prantzos, N.; Abia, C.; Cristallo, S.; Limongi, M.; Chieffi, A. Chemical evolution with rotating massive star yields II. A new assessment of the solar s- and r-process components. *Mon. Not. R. Astron. Soc.* **2020**, *491*, 1832–1850. [\[CrossRef\]](#)
- Busso, M.; Gallino, R.; Wasserburg, G.J. Nucleosynthesis in Asymptotic Giant Branch Stars: Relevance for Galactic Enrichment and Solar System Formation. *Annu. Rev. Astron. Astrophys.* **1999**, *37*, 239–309. [\[CrossRef\]](#)
- Straniero, O.; Gallino, R.; Cristallo, S. S process in low-mass asymptotic giant branch stars. *Nucl. Phys. A* **2006**, *777*, 311–339. [\[CrossRef\]](#)
- Pignatari, M.; Gallino, R.; Heil, M.; Wiescher, M.; Käppeler, F.; Herwig, F.; Bisterzo, S. The Weak s-Process in Massive Stars and Its Dependence on the Neutron Capture Cross Sections. *Astrophys. J.* **2010**, *710*, 1557–1577. [\[CrossRef\]](#)
- Liu, N.; Gallino, R.; Cristallo, S.; Bisterzo, S.; Davis, A.M.; Trappitsch, R.; Nittler, L.R. New Constraints on the Major Neutron Source in Low-mass AGB Stars. *Astrophys. J.* **2018**, *865*, 112. [\[CrossRef\]](#)
- Liu, N.; Stephan, T.; Cristallo, S.; Gallino, R.; Boehnke, P.; Nittler, L.R.; Alexander, C.M.; Davis, A.M.; Trappitsch, R.; Pellin, M.J.; et al. Presolar Silicon Carbide Grains of Types Y and Z: Their Molybdenum Isotopic Compositions and Stellar Origins. *Astrophys. J.* **2019**, *881*, 28. [\[CrossRef\]](#)
- Cristallo, S.; Piersanti, L.; Straniero, O.; Gallino, R.; Domínguez, I.; Käppeler, F. Asymptotic-Giant-Branch Models at Very Low Metallicity. *Publ. Astron. Soc. Aust.* **2009**, *26*, 139–144. [\[CrossRef\]](#)

15. Choplin, A.; Siess, L.; Goriely, S. The intermediate neutron capture process. I. Development of the i-process in low-metallicity low-mass AGB stars. *Astron. Astrophys.* **2021**, *648*, A119. [[CrossRef](#)]
16. Denissenkov, P.A.; Herwig, F.; Woodward, P.; Andrassey, R.; Pignatari, M.; Jones, S. The i-process yields of rapidly accreting white dwarfs from multicycle He-shell flash stellar evolution models with mixing parametrizations from 3D hydrodynamics simulations. *Mon. Not. R. Astron. Soc.* **2019**, *488*, 4258–4270. [[CrossRef](#)]
17. Choplin, A.; Tominaga, N.; Meyer, B.S. A strong neutron burst in jet-like supernovae of spinstars. *Astron. Astrophys.* **2020**, *639*, A126. [[CrossRef](#)]
18. Pignatari, M.; Hoppe, P.; Trappitsch, R.; Fryer, C.; Timmes, F.X.; Herwig, F.; Hirschi, R. The neutron capture process in the He shell in core-collapse supernovae: Presolar silicon carbide grains as a diagnostic tool for nuclear astrophysics. *Geochim. Cosmochim. Acta* **2018**, *221*, 37–46. [[CrossRef](#)]
19. Giuliani, S.A.; Martínez-Pinedo, G.; Wu, M.R.; Robledo, L.M. Fission and the r -process nucleosynthesis of translead nuclei in neutron star mergers. *Phys. Rev. C* **2020**, *102*, 045804. [[CrossRef](#)]
20. Fiore, S.; Aberle, O.; Angelone, M.; Calviani, M.; Di Giambattista, F.; Lepore, L.; Nyman, M.; Pillon, M.; Plompen, A. Self Powered Neutron Detectors with High Energy Sensitivity. *Eur. Phys. J. Web Conf.* **2020**, *225*, 02001. [[CrossRef](#)]
21. Reifarh, R.; Erbacher, P.; Fiebiger, S.; Göbel, K.; Heftrich, T.; Heil, M.; Käppeler, F.; Klapper, N.; Kurtulgil, D.; Langer, C.; et al. Neutron-induced cross sections. From raw data to astrophysical rates. *Eur. Phys. J. Plus* **2018**, *133*, 424. [[CrossRef](#)]
22. Massimi, C.; Domingo-Pardo, C.; Vannini, G.; Audouin, L.; Guerrero, C.; Abbondanno, U.; Aerts, G.; Álvarez, H.; Álvarez-Velarde, F.; Andriamonje, S.; et al. Au197(n,γ) cross section in the resonance region. *Phys. Rev. C* **2010**, *81*, 044616. [[CrossRef](#)]
23. Massimi, C.; Becker, B.; Dupont, E.; Kopecky, S.; Lampoudis, C.; Massarczyk, R.; Moxon, M.; Pronyaev, V.; Schillebeeckx, P.; Sirakov, I.; et al. Neutron capture cross section measurements for <sup>197</sup>Au from 3.5 to 84 keV at GELINA. *Eur. Phys. J. A* **2014**, *50*, 124. [[CrossRef](#)]
24. Lederer, C.; Colonna, N.; Domingo-Pardo, C.; Günsing, F.; Käppeler, F.; Massimi, C.; Mengoni, A.; Wallner, A.; Abbondanno, U.; Aerts, G.; et al. Au197(n,γ) cross section in the unresolved resonance region. *Phys. Rev. C* **2011**, *83*, 034608. [[CrossRef](#)]
25. Gawlik-Ramiega, A.; Lederer-Woods, C.; Krčička, M.; Valenta, S.; Battino, U.; Andrzejewski, J.; Perkowski, J.; Aberle, O.; Audouin, L.; Bacak, M.; et al. Measurement of the <sup>76</sup>Ge(n,γ) cross section at the n\_TOF facility at CERN. *Phys. Rev. C* **2021**, *104*, 044610. [[CrossRef](#)]
26. Amaducci, S.; Colonna, N.; Cosentino, L.; Cristallo, S.; Finocchiaro, P.; Krčička, M.; Massimi, C.; Mastromarco, M.; Mazzone, A.; Mengoni, A.; et al. First Results of the <sup>140</sup>Ce(n,γ)<sup>141</sup>Ce Cross-Section Measurement at n\_TOF. *Universe* **2021**, *7*, 200. [[CrossRef](#)]
27. Cristallo, S.; Abia, C.; Straniero, O.; Piersanti, L. On the Need for the Light Elements Primary Process (LEPP). *Astrophys. J.* **2015**, *801*, 53. [[CrossRef](#)]
28. Watson, D.; Hansen, C.J.; Selsing, J.; Koch, A.; Malesani, D.B.; Andersen, A.C.; Fynbo, J.P.U.; Arcones, A.; Bauswein, A.; Covino, S.; et al. Identification of strontium in the merger of two neutron stars. *Nature* **2019**, *574*, 497–500. [[CrossRef](#)]
29. Busso, M.; Gallino, R.; Lambert, D.L.; Travaglio, C.; Smith, V.V. Nucleosynthesis and Mixing on the Asymptotic Giant Branch. III. Predicted and Observed s-Process Abundances. *Astrophys. J.* **2001**, *557*, 802–821. [[CrossRef](#)]
30. D'Orazi, V.; Campbell, S.W.; Lugaro, M.; Lattanzio, J.C.; Pignatari, M.; Carretta, E. On the internal pollution mechanisms in the globular cluster NGC 6121 (M4): Heavy-element abundances and AGB models. *Mon. Not. R. Astron. Soc.* **2013**, *433*, 366–381. [[CrossRef](#)]
31. Liu, N.; Savina, M.R.; Gallino, R.; Davis, A.M.; Bisterzo, S.; Gyngard, F.; Käppeler, F.; Cristallo, S.; Dauphas, N.; Pellin, M.J.; et al. Correlated strontium and barium isotopic compositions of acid-cleaned single mainstream silicon carbides from Murchison. *Astrophys. J.* **2015**, *803*, 12. [[CrossRef](#)]
32. Vescovi, D.; Cristallo, S.; Busso, M.; Liu, N. Magnetic-buoyancy-induced Mixing in AGB Stars: Presolar SiC Grains. *Astrophys. J. Lett.* **2020**, *897*, L25. [[CrossRef](#)]
33. Domoto, N.; Tanaka, M.; Wanajo, S.; Kawaguchi, K. Signatures of r-process Elements in Kilonova Spectra. *Astrophys. J.* **2021**, *913*, 26. [[CrossRef](#)]
34. Tagliente, G.; Milazzo, P.M.; Fujii, K.; Abbondanno, U.; Aerts, G.; Álvarez, H.; Álvarez-Velarde, F.; Andriamonje, S.; Andrzejewski, J.; Audouin, L.; et al. Neutron capture on Zr94: Resonance parameters and Maxwellian-averaged cross sections. *Phys. Rev. C* **2011**, *84*, 015801. [[CrossRef](#)]
35. Simonits, A.; De Corte, F.; Van Lierde, S.; Pommé, S.; Robouch, P.; Eguskiza, M. The k0 and Q0 Values for the Zr-Isotopes: A Re-Investigation. *J. Radioanal. Nucl. Chem.* **2000**, *245*, 199–203. [[CrossRef](#)]
36. Porzio, C.; Michelagnoli, C. High-precision spectroscopy of <sup>65</sup>Ni via neutron capture. *IL Nuovo Cimento C* **2021**, *44*, 69. [[CrossRef](#)]
37. Wang, T.; Lee, M.; Kim, G.; Oh, Y.; Namkung, W.; Ro, T.I.; Kang, Y.R.; Igashira, M.; Katabuchi, T. Measurement of keV-neutron capture cross-sections and capture γ-ray spectra of <sup>56</sup>Fe and <sup>57</sup>Fe. *Nucl. Instrum. Methods Phys. Res. B* **2010**, *268*, 440–449. [[CrossRef](#)]
38. Pignatari, M.; Zinner, E.; Bertolli, M.G.; Trappitsch, R.; Hoppe, P.; Rauscher, T.; Fryer, C.; Herwig, F.; Hirschi, R.; Timmes, F.X.; et al. Silicon Carbide Grains of Type C Provide Evidence for the Production of the Unstable Isotope <sup>32</sup>Si in Supernovae. *Astrophys. J.* **2013**, *771*, L7. [[CrossRef](#)]
39. Fujiya, W.; Hoppe, P.; Zinner, E.; Pignatari, M.; Herwig, F. Evidence for Radiogenic Sulfur-32 in Type AB Presolar Silicon Carbide Grains? *Astrophys. J.* **2013**, *776*, L29. [[CrossRef](#)]